

# Realtime Compilation for Continuous Angle Quantum Error Correction Architectures

Sayam Sethi  
Department of Electrical and  
Computer Engineering  
University of Texas at Austin  
sayams@utexas.edu

Jonathan M. Baker  
Department of Electrical and  
Computer Engineering  
University of Texas at Austin  
jonathan.baker@austin.utexas.edu

**Abstract**—Quantum error correction (QEC) is necessary to run large scale quantum programs. Regardless of error correcting code, hardware platform, or systems architecture, QEC systems are limited by the types of gates which they can perform efficiently. In order to make the base code’s gate set universal, they typically rely on the production of a single type of resource state, commonly T, in a different code which is then distilled and injected into the base code. This process is neither space nor time efficient and can account for a large portion of the total execution time and physical qubit cost of any program. In order to circumvent this problem, alternatives have been proposed, such as the production of continuous angle rotation states [1], [6]. These proposals are powerful because they not only enable localized resource generation but also can potentially reduce total space requirements.

However, the production of these states is non-deterministic and can require many repetitions in order to obtain the desired resource. The original proposals suggest architectures which do not actively account for realtime management of its resources to minimize total execution time. Without this, static compilation of programs to these systems will be unnecessarily expensive. In this work, we propose a realtime compilation of programs to these continuous angle systems and a generalized resource sharing architecture which actively minimizes total execution time based on expected production rates. To do so, we repeatedly redistribute resources on-demand which depending on the underlying hardware can cause excessive classical control overhead. We further address this by dynamically selecting the frequency of recompilation. Our compiler and architecture improves over the baseline proposals by an average of  $2\times$ .

## I. INTRODUCTION

Quantum error correction is necessary in order to execute large scale applications. As we scale, quantum resources will be relatively scarce and it is critical to develop realtime management of these resources in order to maximize the value of available hardware. These resources include classical bandwidth for decoding [28], ancilla management for communication and decompositions [9], and the creation and use of special resource states called *magic states* [8], [24]. The study of these resources has been concentrated around surface codes as a promising candidate error correction code for small to

intermediate scale quantum hardware [12], [23] due to its limited hardware connectivity, high threshold, and well studied decoding procedures.

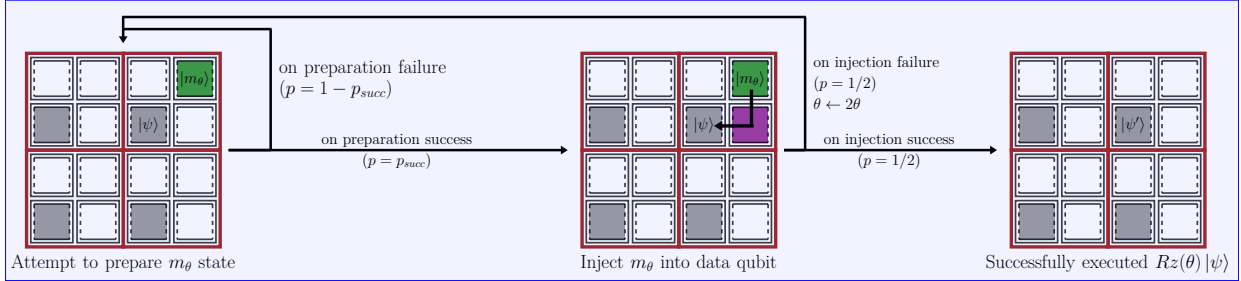
Critical to the success of any quantum error correcting code is providing support for the creation and consumption of *magic states* (or resource states). Since no code natively supports a transversal and universal gate set [10], there must be some gates that are performed in *another* code and converted or distilled into special states that can be used to apply that gate in the original code. For example, in the surface code we natively only support the Clifford gates (e.g. CNOT, X, Z, and H) which are not universal. One common way to make this gate set universal is to produce T states and inject them as necessary. It is also typical that we only support a finite gate set and not a continuous one. For example, most physical quantum computers can support  $Rz(\theta)$  for any  $\theta$ , but the surface code only supports a discrete set. By adding in the T gate to the Clifford set we get a universal gate set since we can approximate any  $Rz(\theta)$  gate to an arbitrary precision [29]. Unfortunately, this type of synthesis results in circuits which are extremely long and require large numbers of bulky *factories* to produce the magic states; both space and time requirements for any circuit become dominated by T state production.

Recently, several alternative approaches have been proposed [1], [6], which rather than requiring magic state factories to create one fixed type of  $Rz$  rotation, instead propose methods to create analog rotation states  $|m_\theta\rangle$ , adopting the syntax from [1]. When injecting this state we can perform an arbitrary  $Rz(\theta)$  rotation. This is especially powerful because it ideally reduces the total space requirement for producing non-Clifford gates. We can use ancilla qubits local to the injection site to prepare the necessary  $|m_\theta\rangle$  in contrast to distilling hundreds or thousands of T gates per  $Rz$  rotation [30]. There is limited architectural support for this strategy specifically for the realtime management of the nondeterministic behavior of the  $|m_\theta\rangle$  production. In the original proposal from [1], their STAR architecture provides a basic structure to demonstrate the technique’s efficacy, but 1. limits state production to atomic STAR patches (see Figure 1) which

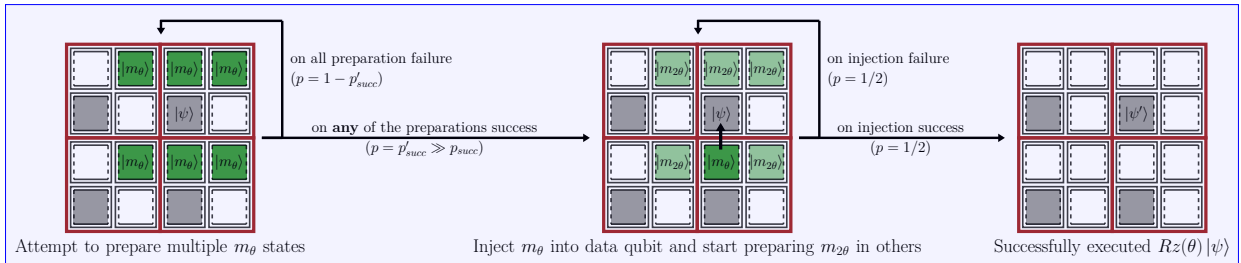


(a) Example data qubit and magic state as surface code tiles

(b) Grid of atomic STAR blocks as defined in [1]



(c) Protocol for the baseline architecture



(d) Protocol for the dynamic architecture (this work)

Fig. 1: (a, top) Surface Code data qubit with labeled X and Z edges. Gate execution depends on the correct exposure of these edges to ancilla channels. (a, bottom) A prepared  $|m_\theta\rangle$  state converted to Surface Code. (b) Baseline STAR architecture from [1] with three ancilla (white) for every data qubit (dark grey) with prepared rotation states labeled (green). Four star patches are outlined in red. (c) The baseline repeat-until-success (RUS) protocol which always attempts preparation of  $|m_\theta\rangle$  in the upper right ancilla of the atomic STAR patch. On success, injection can proceed, otherwise we attempt to prepare again. If injection fails, we prepare a  $2\theta$  fixup and start from the beginning. (d) In our dynamic compilation scheme we attempt multiple preparations in parallel reducing the number of restarts. During injection, we preemptively attempt to prepare any fixups reducing stalls from restarting the entire process.

limits parallel production when other space is unused and 2. does not directly adapt program execution as a function of the highly non-deterministic state production.

In this work, we provide an improved compilation scheme for continuous angle rotation architectures. In our compilation technique, we consider the ancillas independent of the data qubit, allowing for sharing of resources between multiple qubits and gates. This necessitates making decisions on the dynamic assignment of ancilla since allocating more ancilla for a particular gate operation reduces the expected time to prepare  $|m_\theta\rangle$  but constrains the execution of neighboring gates, but allocating fewer ancilla leads to inefficient utilization of the resources. To counter this problem, we provide a mechanism to dynamically manage the ancilla that are available for different gate operations, including but not limited to  $Rz$

and CNOT gates. This approach allows us to flexibly allocate ancilla. We also propose a space-time efficient technique that schedules the long-distance gate operations while minimizing the wait time. We achieve an average improvement of  $2\times$  over a statically compiled execution, even after accounting for classical overheads during dynamic compilation to recompute the best ancilla use. Our approach can be directly incorporated in any quantum architecture involving non-deterministic execution and/or variable ancilla availability.

The primary contributions of this work are

- 1) An open source [31] efficient compilation scheme for quantum error correction systems which support native continuous angle resource states. We improve over baseline proposals by an average of  $2\times$  in total program execution time.

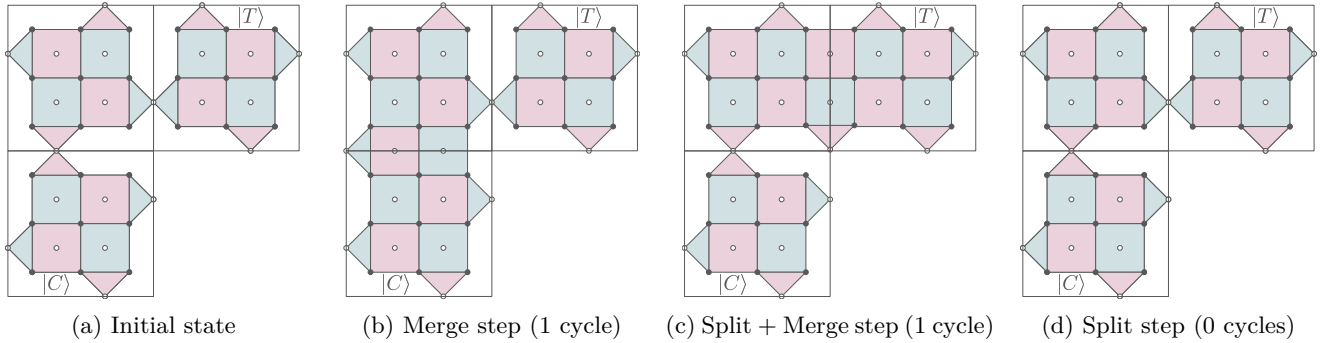


Fig. 2: Execution of a CNOT gate in lattice surgery using exactly 2 steps. In each step, we have three surface code qubits (of  $d = 3$ ) indicated by the squares. Here the CNOT is performed between  $|C\rangle$  as the control and  $|T\rangle$  as the target with a single ancilla patch in between on the top-left. Note that the horizontal edges are the  $Z$  edges (all red) and the vertical edges are the  $X$  edges (all blue, as labeled in Figure 1). In general, this patch can be arbitrarily long and shaped so long as the correct boundaries are adjacent. We assume ancilla preparation is done ahead of time.

- 2) Compilation which directly accounts for the inherent non-deterministic behavior of continuous angle resource state production; we introduce the notion of real-time recompilation depending on the prior success of production and consumption of these states.
- 3) An improved architecture for local resource state production which reduces total space (ancilla) requirements while simultaneously reducing the total runtime of programs on these systems. Even in the most constrained architectures, our compilation method results in an average  $1.65\times$  improvement.
- 4) Real system measurement latencies restrict the amount and frequency of classical recompilation that can occur without incurring excessive idling on the quantum system; our compilation scheme easily adapts to any hardware platform and dynamically selects the frequency of recompilation: to our knowledge, the first of its kind to do so. This real-time control consideration is extensible to other QEC systems.

## II. BACKGROUND AND RELATED WORK

Scalable quantum computation requires error correction in order to achieve *logical error rates* sufficiently low for successful program execution. We focus on Surface Codes a code with many attractive properties for available or soon-to-be available hardware platforms. Surface codes require only nearest neighbor connectivity between physical qubits, its parity checks require only 4 two qubit gates, it has a high threshold and it has well-studied decoders [11], [13]. Surface code architectures are also fairly well studied with the most popular being the rotated surface code with lattice surgery operations [15], [23]. The rotated surface code is a  $d \times d$  patch of qubits with  $O(d^2)$  data qubits and ancilla qubits, where  $d$  is the distance of the code. The patch is composed of  $X$  checks and  $Z$  checks which collect syndromes about  $X$  and  $Z$  errors, respectively. The boundaries of the square patch are either  $X$  or  $Z$  edges

which determine how the logical qubit can interact with other qubits. Figure 2 shows three such surface code tiles for  $d = 3$  (each black outlined square).

Surface code architectures are a fabric of many  $d \times d$  sized tiles where program qubits are mapped onto these tiles. Tiles can be deformed fairly arbitrarily so long as the distance of the shortest path between any pair of corresponding edges (e.g.  $X$  edge to another  $X$  edge) is always at least  $d$ . Deformation, amongst other operations, is one of many available operations in a surface code architecture and can be used to transport information from one region of the device to another in order to interact with other distant logical qubits. In order to do so, the grid of tiles must allocate some number of logical *ancilla*. In order to interact two logical qubits, we employ lattice surgery using intermediate ancilla. For a more complete coverage of these operations, we refer to [23].

We summarize the necessary information for this work:

- Program qubits are assigned to a single  $d \times d$  tile in the larger fabric, e.g. using AutoBraid [16].
- The logical operation CNOT (Figure 2) occurs in **two** steps: a) measure the  $ZZ$  operator between the control and the ancilla followed by b) measure the  $XX$  operator between the ancilla and the target.
- Interactions between logical qubits use a contiguous path of ancilla qubits which must touch every interacting qubit.
- A special type of multi-qubit interaction, or *Pauli-product measurement* as in Figure 6a, can in **one** step by interacting the  $P$ -edge of each interacting logical qubit to an intermediate ancilla channel contiguous between each, where  $P$  is the specific Pauli. For example, a  $ZZ$  Pauli product measurement can be done by interacting the  $Z$  edge of qubit 1 and the  $Z$  edge of qubit 2 to one contiguous block of ancilla. This can be done in 1 step regardless of distance between them, so long as the ancilla channel is contiguous.

### A. Resource State Distillation

In order to make universal gate sets for quantum error correction codes, additional resource states (for example  $|T\rangle$  or T states which can be used to perform logical T gates via teleportation) are prepared remotely in a different code which does admit a transversal implementation. Preparation of these states can fail and are prepared with some fixed logical error rate which is different from the logical error rate of the base code. Through a process of distillation more error prone states can be used to generate lower logical error rate versions. Resource states are usually prepared remotely in factories and consumed on demand by the program. The total space-time cost of factory distillation in some estimates can take upwards of 90% of the total space-time volume of the program’s execution [14].

### B. Continuous Angle Rotation Architectures

Recent works [1], [6] have proposed fault-tolerant architectures to prepare arbitrary small angle rotation gates with low overheads and small logical error rates. The typical architecture for QEC systems is to have the primary *computational* code which maintains all data qubits and external factory regions which produce special resource states of a single variety, usually  $|T\rangle$  for surface codes. It has been acknowledged that T count and depth dominate resource costs in both space and time [24]. Alternative proposals have appeared including code switching [2], higher dimensional codes [19] and most recently these “small-angle” synthesis procedures [1], [6] which propose repeat-until-success (RUS) procedures for the production of *arbitrary* magic states  $|m_\theta\rangle$  which can be injected to perform  $Rz(\theta)$  (Figure 1) directly without the need for expensive decompositions or distillation with varying success. The total space-time cost of these procedures is appealing for near and intermediate term demonstrations of error correction by severely reducing total physical qubit requirements necessary for distillation factories. These works propose simple versions of architectures which support their RUS strategies, but they are limited in scale and lack a full compiler to optimize for the non-deterministic behavior of their techniques, which even in other literature has gone largely ignored.

We focus on the technique and architecture proposed in [1] which uses a  $[[4, 1, 1, 2]]$  error *detection* code to produce the  $|m_\theta\rangle$  which can be embedded into the larger surface code architecture multiple times as in Figure 3. This preparation can be abstracted out as a non-deterministic preparation with appropriate probability of success as shown in Figure 1. They give three examples of simple architectures which localize the production of these states: 1. STAR block, a  $2 \times 2$  grid of surface code tiles 1 of which is data, and 1 of which produces the resource state, and 2 ancilla used for communication, 2. Compact STAR block, a  $3 \times 1$  grid with 1 data and 2 ancilla and 3. Compressed STAR block, a  $2 \times 1$  grid with 1 data and 1 ancilla. This

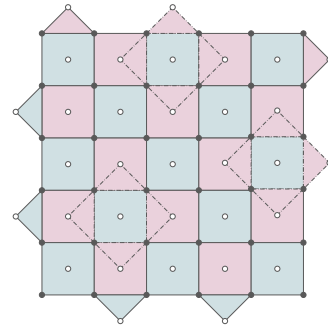


Fig. 3: Parallel preparation of the  $|m_\theta\rangle$  state within a surface code patch of distance 5. Each sub-patch enclosed by the dotted lines represent a single sub-patch of a  $[[4, 1, 1, 2]]$  error detection code. Multiple of these sub-patches can be constructed within a single surface code patch (as shown in the figure by the three disjoint sub-patches). Each sub-patch attempts to prepare a  $|m_\theta\rangle$  state in an RUS fashion. Whenever any sub-patch succeeds, it attempts to expand the state to the entire surface code patch and destroys other sub-patches in the process. If the expansion fails, the entire process is restarted. For a more detailed explanation of the protocol, refer [1].

atomic abstraction is unnecessary and a more complete compiler (this work) can better manage ancilla to both create local and remote magic states and allocate ancilla for communication.

### C. Prior Compilation Work

There are two primary categories for compilation for quantum systems: 1) *physical* compilation focused on the implementation of physical gates on individual physical qubits and 2) *logical* compilation focused on the management of *logical* qubits. The first is typically defined by the constraints of the underlying hardware for which several works have focused on tailoring efficient execution of physical syndrome extraction circuits to the hardware properties e.g. superconducting qubits [36], trapped ions [20] and neutral atoms [17], [34]. These are often distinct from generalized compilers [22], [26], [32] because of the simple and repetitive nature of the underlying circuits.

We focus on the second type of compilation. As QEC codes, and surface codes in particular, become more realistically implementable, several general purpose compilers [3], [16], [18], [23], [25], [35] have emerged, typically focusing on problems related to path finding and logical qubit routing. However, these all suffer from the notable exception that they are static. These are also typically distinct from the synthesis problem designed to convert circuits into versions using only gates from the limited universal gate set, such as in [30]. We focus on small-angle rotation synthesis which is a different approach than prior works focused on Clifford+T and focus optimizations on reducing T requirements from synthesis [4], [5].

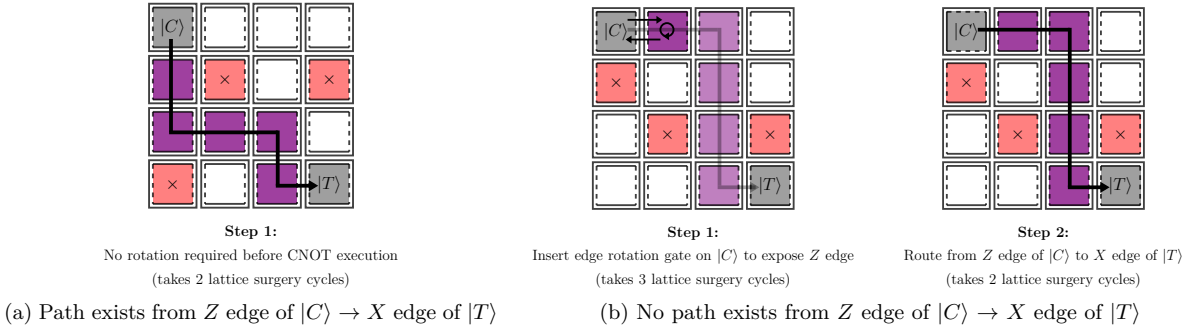


Fig. 4: Two different possible scenarios for CNOT execution in the lattice surgery grid. The qubits colored in red and marked with a cross ( $\times$ ) are busy and/or unavailable for routing the CNOT gate. Recall from Figure 1a that the solid edges are the  $Z$  edges and the dotted edges are the  $X$  edges. CNOT execution in (a) requires only 2 lattice surgery cycles in contrast with (b) which requires a total of 5 cycles.

### III. REALTIME COMPILATION FOR CONTINUOUS ANGLE ROTATION ARCHITECTURES

In this section, we discuss the compilation of high level programs to surface code architectures which support Clifford+Rz gates as opposed to the traditional Clifford+T. We assume all programs have already been synthesized into the appropriate gate set. As opposed to typical distillation factory architectures, in small angle rotation architectures, only small seeds of  $|m_\theta\rangle$  states are prepared and expanded locally into surface code qubits. It takes at most a single logical patch for preparation at the cost of additional uncertainty in its preparation time. In prior work, atomic units of data qubits and ancilla for the preparation of single qubit gates are used. We propose a much more flexible architecture which allows ancilla to be reused and allocated for various rotations dynamically.

#### A. Execution of CNOT Gate

Lattice surgery on surface codes provides a convenient way to perform CNOT gates between two data qubits that can be arbitrarily far apart in constant time (taking 2 lattice surgery cycles as shown in Figure 2). The only requirements for the execution is that there should exist a path of ancilla qubits connecting the control to the target (via at least one ancilla qubit), and the path should be from the  $Z$  edge of the control qubit to the  $X$  edge of the target qubit. It might be possible that such a path does not exist, either due to the ancilla being occupied for another gate operation, or the required edges ( $X$  or  $Z$  edges) of the data qubit not having any neighboring ancilla. In such cases, the compiler would need to insert an edge-rotation gate to orient the correct edge of the qubit onto the chosen path. This gate operation requires one free adjacent ancilla qubit and takes 3 lattice surgery cycles. Figure 4 shows an example for both situations.

The routing algorithm and path selection are crucial to an optimal compilation scheme. Multiple path finding techniques have been proposed in literature, such as shortest path selection [18] and AutoBraid [16], however, they

don't account for non-deterministic ancilla activity and edge-rotation gates. As a result, these techniques do not permit 'early' start of the next set of gates if any gate in the current layer takes longer to execute. For instance, if two CNOTs are scheduled to execute simultaneously with one CNOT taking 2 cycles and the other taking 5 cycles, the next set of gates will only be scheduled after the CNOT gate taking 5 cycles is finished. However, some of the gates in the next layer can start after the CNOT gate taking 2 cycles finishes. This problem is amplified when we have non-deterministic  $Rz$  gates, which we discuss in more detail in Section III-B.

As evident from Figure 5, for AutoBraid, a large percentage of the CNOT gates take 5 and 8 cycles to execute (8 cycles are taken when there is a single ancilla connecting the control and target, and edges for both the control and target are incorrect, thus requiring  $3 + 3 + 2$  cycles: edge-rotation of the control followed by the target followed by the CNOT), in contrast to our dynamic protocol where more than 50% of the CNOT gates take 2 cycles and more than 90% of CNOTs take 6 or less cycles. Here, we only consider the time taken after the gate is scheduled.

Because AutoBraid and other static compilation schemes only schedule the next set of gates once all gates in the current scheduled set are completed, this increases the idling time of the qubits. This is required for static compilation because we can't know the state of non-deterministic procedures ahead of time. For dynamic, we attempt to schedule the next gate operation immediately when the previous gate operation on the data qubit is finished. Thus, even though CNOT gates might have been scheduled, they cannot start immediately since the ancillas required for the CNOT might be busy executing a different gate, as can be seen from the continuous distribution of the cycles taken for the dynamic compilation scheme. The only time we do not schedule the next gate is when we have to execute a CNOT gate on the control qubit but the target qubit is still busy, or vice versa.

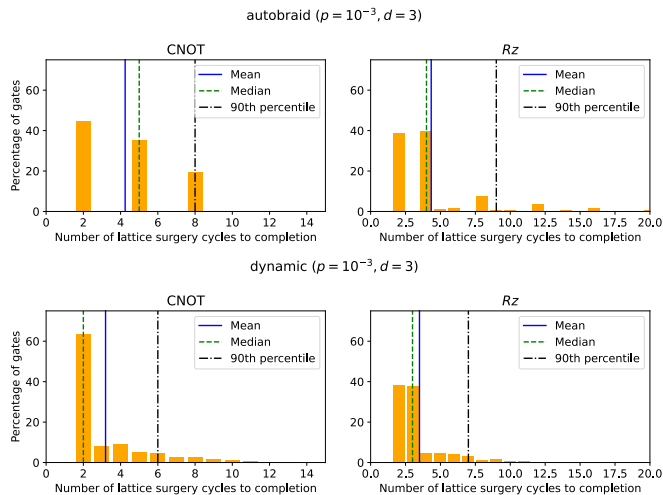


Fig. 5: Histograms showing the time taken for CNOT and  $Rz$  gates (including all correction gates) to complete *after they are scheduled* (accumulated over all benchmarks).

### B. Execution of $Rz(\theta)$ Rotation Gate

We summarize the discussion in Section II-B regarding the protocol to execute  $Rz(\theta)$  rotation gates. The  $Rz(\theta)$  rotation gate is executed in two steps, 1. preparation of an ancilla qubit in the state  $|m_\theta\rangle$  (as shown in Figure 3), and 2. injection of the  $|m_\theta\rangle$  state into the data qubit and measurement. As discussed in [1], there are two potential injection strategies, shown in Figure 6a and Figure 6b which we refer to as the ZZ injection (substituting  $P = Z$ ) and CNOT injection strategies, respectively. The differences between the two strategies is shown in Table I. Both these injection strategies involve a measurement which outputs +1 and -1 with **equal** probability. We refer to an output of -1 as a failure.

If the measurement output signifies a failure (with fixed probability 1/2), a correction  $Rz(2\theta)$  is required. If this correction fails, another correction gate  $Rz(4\theta)$  is required and so on, as Repeat-Until-Success (RUS). Failed injection means an  $Rz(-\theta)$  gate was executed so executing an  $Rz(2\theta)$  correction gate would yield the proper rotation. However, since  $Rz(2\theta)$  is likely a non-Clifford, we must repeat. In general, if an  $Rz(2^k\theta)$  injection fails we require  $Rz(2^{k+1}\theta)$  correction. Every injection fails with probability 1/2, hence

$$\begin{aligned} \mathbb{E}[\text{Num. Injections}] &= \sum_{k=1}^{\infty} k \cdot \Pr[k-1 \text{ Failures, 1 Success}] \\ &= \sum_{k=1}^{\infty} \frac{k}{2^k} = 2 \end{aligned}$$

If  $Rz(2^k\theta)$  is a Clifford for some  $k$  (for example consider T or  $\sqrt{T}$ ), this expectation will be  $< 2$  since it will no longer require an injection step. There are two potential strategies for injection, summarized in Section II,

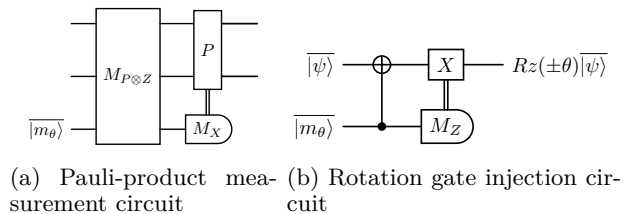


Fig. 6: Circuits for different injection strategies.

Parameter	CNOT	ZZ
Exposed edge	X	Z
Number of ancillas required	2	1
Lattice surgery cycles needed for injection	2	1

TABLE I: Difference between the two injection strategies. The injection in Figure 1c is an example of a CNOT injection and in Figure 1d is an example of a ZZ injection.

one using a CNOT and one using a ZZ Pauli-product measurement. In either case, the compiler must allocate a contiguous block of ancilla. Our compiler reserves ancilla and generates a schedule for each ancilla dynamically determining when its free; we simply require that some path between  $|m_\theta\rangle$  and target all be free at some time.

The preparation of the rotation states  $|m_\theta\rangle$  is itself non-deterministic and is prepared in an ancilla patch. Consequently, assigned ancilla are claimed for an indeterminate number of cycles until the state is prepared correctly. Different states  $|m_\alpha\rangle$  and  $|m_\beta\rangle$  require disjoint ancilla for preparation. Multiple ancilla can be assigned for the preparation of any individual state and any additional successful preparations can be discarded if necessary. The number of ancilla dedicated to the production of a particular state  $|m_\theta\rangle$  can dynamically change. For example, if  $n$  ancilla are assigned in cycle 1 and each fails, wherein some  $m$  of these ancilla are needed for other operations, we can reclaim them and try to prepare the state using  $n - m > 0$  ancilla in the next cycle. Non-deterministic preparation implies that the exact cycle in which consumption can occur at is unknown ahead of time, motivating eager preparation. Our dynamic compilation scheme decides 1. which ancilla are good candidates for preparation (and injection), and 2. when to start preparation, since beginning preparation too early would prevent the ancilla from being used for other gates while waiting for the data qubit. Conversely, starting preparation too late would stall the gate execution. Making informed and intelligent decisions is clearly beneficial as seen in Figure 5. The baseline scheme only attempts to prepares a single  $|m_\theta\rangle$  state and does not perform eager preparation of the correction state. Our dynamic scheme attempts to prepare multiple  $|m_\theta\rangle$  states in parallel and begins eager preparation of the  $|m_{2\theta}\rangle$  correction state during the injection of the  $|m_\theta\rangle$  state.

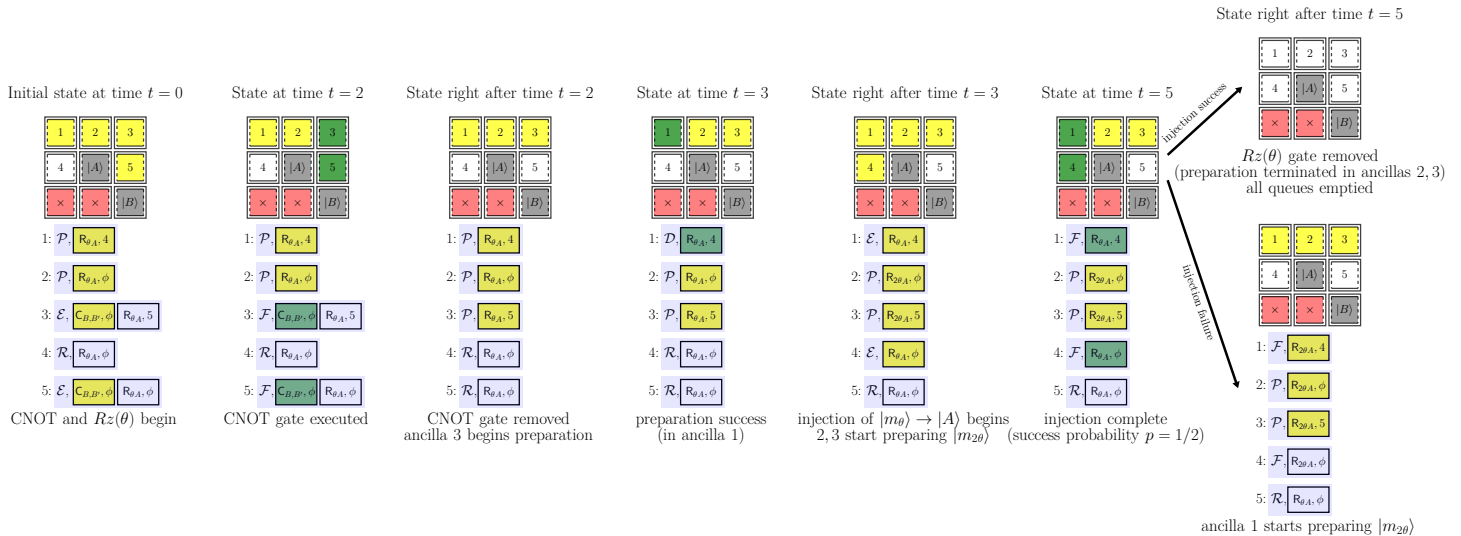


Fig. 7: An example of how the queue is modified and used as the program execution progresses by showing a small section of the larger surface code grid. The CNOT gate is with a target qubit  $|B'\rangle$  (not present). The ancillas coloured in red and marked by a cross ( $\times$ ) are assumed to be unavailable to simplify the example. For this example, the CNOT gate is added to the queue before the  $R_z$  gate. In our actual implementation, however, if multiple gates must be scheduled simultaneously, ties are resolved by prioritizing gates for qubits that have larger circuit depth (since they are more likely to be on the critical path).

#### IV. DYNAMIC COMPILATION FRAMEWORK

Our proposal relies on two dynamically constructed and modified data structures throughout execution: 1. a queue for every ancilla qubit in the system and 2. a minimum-spanning-tree (MST) weighted by historical use for selecting routing paths based on expected availability. We give a high level and then details in subsequent sections.

For each ancilla, we dynamically construct a queue to track not only which operation the ancilla is participating in but what its action or role is in that operation. For example, an ancilla may be used for a routing path or a rotation state preparation. Operations may request many of the same ancilla and compete for shared resources; the order of allocation is significant to prevent wasted resources or race conditions. We maintain a queue for each ancilla qubit and each node of the queue consists of the data structure containing information about the role of the ancilla for the corresponding gate operation. We discuss the exact implementation of the queue in Section IV-A.

Another key component of our dynamic compilation framework is the routing protocol. Choosing an optimal path for each CNOT that minimizes the total program execution time is inherently a computationally intensive problem, even if done statically and all gates take deterministic execution times [16]. We maintain an MST of ancilla throughout computation and update its weights dynamically. To determine the best path for each CNOT in realtime, we query the MST and compute the set of ancilla which is most likely free earliest. We discuss the specifics and its implementation in Section IV-B.

#### A. Managing Ancilla Operations

Variable	Purpose	Possible Values
<i>gate</i>	the gate that the ancilla qubit will help to execute	$C_{p,q}$ : CNOT gate from qubit $p$ (control) onto qubit $q$ (target)
		$R_{\theta p}$ : $R_z(\theta)$ rotation gate on qubit $p$
		$H_p$ : Hadamard gate on qubit $p$
		$E_p$ : edge rotation gate on qubit $p$
<i>helper</i>	other ancilla qubits required	$\phi$ : none $i$ : ancilla qubit $i \in \mathbb{A}$ (required when injecting $ m_\theta\rangle$ via a CNOT)
	<i>status</i>	the current status of the ancilla
$\mathcal{E}$ : executing the top of queue		
$\mathcal{P}$ : preparing $ m_\theta\rangle$ state for the $R_z(\theta)$ gate at top of queue		
$\mathcal{D}$ : done preparing $ m_\theta\rangle$ state and ready to execute $R_z(\theta)$ gate at top of queue		
		$\mathcal{F}$ : finished executing the gate at top of the queue

TABLE II: Variables stored in each node of the queue that contains information about the associated gate. The *status* is associated only with the top node of the queue.

Table II contains the list of variables necessary to determine the operations the ancilla qubit will perform for the gate's execution. Along with storing the gate and the data qubit it acts upon, we store a helper ancilla if needed for the gate execution. For the execution of a  $R_{\theta p}$  gate, we push the  $R_{\theta p}$  gate into the queue of all the ancilla that are adjacent to the  $Z$  edge of  $p$  (for  $ZZ$  type injection). We also push the gate into queues of ancilla that are diagonally adjacent to  $p$  so that the ancilla along the  $X$  edge of the data qubit can be used for executing CNOT between the ancilla and the data qubit  $p$ . The gate

is pushed into the queue of the ancillas preemptively in order to reduce the time the data qubit spends waiting for the  $|m_\theta\rangle$  state after it is done executing the previous gate. In the example execution shown in Figure 7, for the  $R_{\theta A}$  gate, the corresponding neighbouring ancillas are 1, 2, 3 since ancilla 2 is adjacent to the  $Z$  edge of data qubit  $A$  and ancillas 1, 3 can be connected to  $A$  via ancillas 4, 5 respectively, which are both adjacent to the  $X$  edge of  $A$ . We push the  $R_{\theta p}$  gate into the queue of all three preparing ancillas (1, 2, 3) and both routing ancillas (4, 5).

Intuitively, one might think that pushing the  $R_{\theta p}$  gate into the queues of all *valid* neighbouring ancillas would reduced ancilla availability for other gate operations. However, this will not happen. This is because when the  $R_{\theta p}$  gate is pushed to all *valid* neighbouring ancilla queues, there will already be some gates in the queue that are pending execution and this gate will be at a different position in the queue for each ancilla. The ancilla that has the least gates in its queues will be the first one to start preparing  $|m_\theta\rangle$ . Having the least gates in the queue is a direct indication that this ancilla qubit is not being contended by multiple gate operations and hence it can be prioritized to execute  $R_{\theta p}$ . Using the queue also ensures that the priority of the gates is decided by *seniority*, i.e., gates that have already been added to the queue must have been scheduled earlier and they are executed before the gates that have been added later.

When any of the preparing ancilla succeed, the gate for the other ancilla qubits is modified from  $R_{\theta p}$  to  $R_{2\theta p}$  instead of pushing this new gate to the queue. We update the gate in-place is to avoid the gate from losing its place in the queue. If some other ancilla qubits were already preparing  $|m_\theta\rangle$ , then the preparation is aborted and they instead start preparing  $|m_{2\theta}\rangle$  to ensure that the correction state is available sooner if the injection fails. If the injection does fail, the ancilla qubit that was used to inject  $|m_\theta\rangle$  also begins preparing  $|m_{2\theta}\rangle$ . We attempt to maximize parallel preparation since both the preparation and the injection are done in a RUS fashion, and hence more attempts leads to reduced expectation times. This has also be seen from the smaller mean in Figure 5.

### B. Efficient Path Finding

We use a greedy strategy to find the path for the execution of CNOT gates. To minimize the total program execution time, we choose the path that will finish the earliest. Even if a path exists that starts earlier, it might not *finish* the earliest since this path might require an edge-rotation gate. In an ideal scenario, we would know the exact earliest time each ancilla qubit can be used to route the CNOT gate. This cannot be obtained due to the non-deterministic nature of the  $Rz$  gates. We instead use the *activity* of the ancilla qubits as a measure to determine which ancilla qubits are less *likely* to be available in the near future. The activity of each ancilla qubit is defined

---

### Algorithm 1 CNOT Execution Algorithm

---

```

1: procedure EXECUTE_CNOT_GATE(Queue, Control, Target)
2:   MST  $\leftarrow$  GET_LATEST_COMPUTED_MST_OF_ANCILLAS()
3:   bestStartTime  $\leftarrow$   $\infty$ 
4:   bestPath  $\leftarrow$   $\phi$ 
5:   for all edges  $e_C \in$  NEIGHBOURING_ANCILLAS(Control) do
6:     for all edges  $e_T \in$  NEIGHBOURING_ANCILLAS(Target) do
7:       startTime  $\leftarrow$  0
8:       ancilla_C  $\leftarrow$  GET_ANCILLA( $e_C$ )
9:       ancilla_T  $\leftarrow$  GET_ANCILLA( $e_T$ )
10:      if not IS_X_EDGE( $e_C$ ) then
11:        expFreeTime  $\leftarrow$  GET_EXPECTED_FREE_TIME(ancilla_C)
12:        startTime  $\leftarrow$  MAX(startTime, expFreeTime + 3)
13:      if not IS_Z_EDGE( $e_T$ ) then
14:        expFreeTime  $\leftarrow$  GET_EXPECTED_FREE_TIME(ancilla_T)
15:        startTime  $\leftarrow$  MAX(startTime, expFreeTime + 3)
16:      path  $\leftarrow$  FIND_PATH(MST, ancilla_C, ancilla_T)
17:      for all ancilla  $\in$  path do
18:        expFreeTime  $\leftarrow$  GET_EXPECTED_FREE_TIME(ancilla)
19:        startTime  $\leftarrow$  MAX(startTime, expFreeTime)
20:      if startTime < bestStartTime then
21:        bestStartTime  $\leftarrow$  startTime
22:        bestPath  $\leftarrow$  path  $\cup$   $\{e_C, e_T\}$ 
23:      gate  $\leftarrow$  CNOT_GATE(Control, Target, bestPath)
24:      QUEUE  $\leftarrow$  ADD_GATE_TO_QUEUE(QUEUE, gate)
25:      return QUEUE

```

---

as the normalized value of the number of cycles the ancilla qubit was active in the last  $c$  cycles, i.e.,

$$activity = \frac{\#cycles \text{ active in last } c \text{ cycles}}{c}$$

Using *activity* as the metric, we choose the path that has the smallest maximum activity, since such a path is most likely to have all its ancilla qubits freed the earliest. This can be computed by constructing a weighted undirected graph of the grid with the qubits as the nodes, the edge weights as the max of the activity between the neighbouring qubits. We then compute the Minimum Spanning Tree (MST) of the grid and choose the path between the control and target that lies on this MST. The Minimum Spanning Tree is guaranteed to contain the path between *every pair of vertices* that has the least maximum weight out of every possible path between each pair of vertices [7]. Therefore, we can use the same MST to route CNOT gates between any pairs of qubits.

We want to minimize the *finish* time of the CNOT gate but computing the MST only guarantees that the *start* time is minimized. For this, we consider the expected completion time of each of the 16 paths,  $p_i$ , from control to target (4 neighbors each = 16 paths using the MST of ancilla). For each ancilla  $a \in p_i$  with queue  $Q_a$ , it's expected free time is given as

$$\mathbb{E}[f_a] = \sum_{o \in Q_a} \mathbb{E}[\tau_o]$$

where  $f_a$  is the free time of ancilla  $a$  and  $\tau_o$  is the execution time of operation  $o$ . Then the expected completion time for a given path  $p_i$  is

$$\mathbb{E}[p_i \text{ completes}] = 3r_C + 3r_T + \mathbb{E}[\tau_{CNOT}] + \max_{a \in p_i} \mathbb{E}[f_a]$$



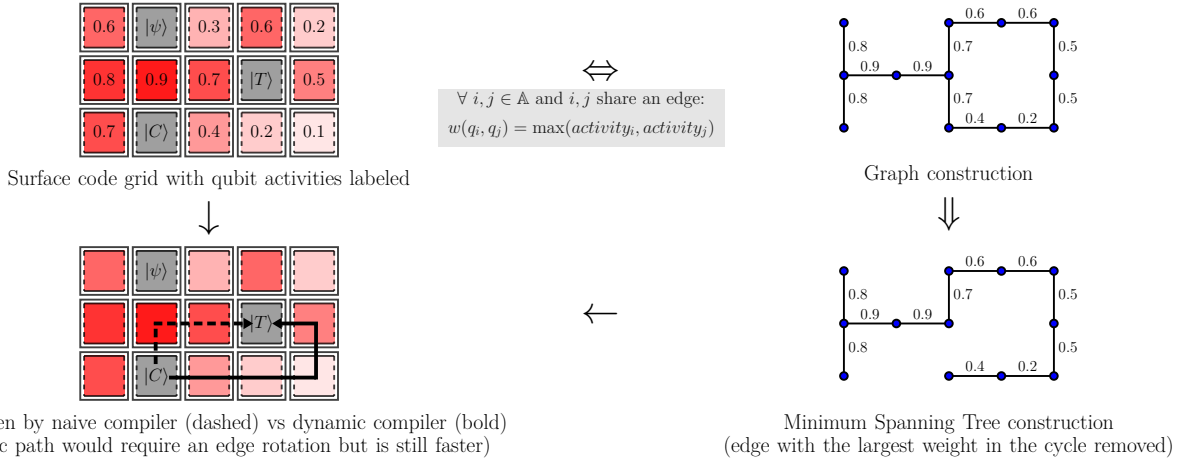


Fig. 8: MST construction protocol and comparison of paths chosen by different compilation schemes. Note that even though the path chosen by Algorithm 1 requires an edge rotation gate, it will take lesser time to execute (in expectation) since all the ancillas along the chosen path are less active and hence their queues will be shorter. The edge rotation gate does not require all ancillas to be free, only the ancilla adjacent to the control needs to be freed.

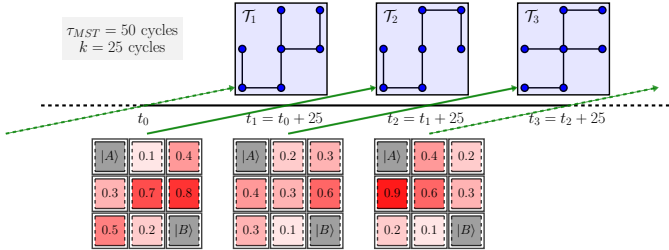


Fig. 9: An example showing the MST computation timeline mid-execution. A new MST computation begins every  $k = 25$  cycles and each MST computation takes  $\tau_{MST} = 50$  cycles. All CNOT operations that are scheduled between time  $t_2$  and  $t_3$  will use the MST  $\mathcal{T}_2$ , whose computation started at  $t_0$  and corresponds to the activity in the grid at time  $t_0$ . Note that this avoids any stalling of the quantum program at the cost of using an MST with *stale* information.

where  $\mathbb{E}[\tau_{CNOT}] = 2$ ,  $r_C, r_T \in \{0, 1\}$  and  $r_C, r_T = 1$  if an edge rotation is necessary for the control or target, respectively. We choose  $\min_{p_i} \mathbb{E}[p_i \text{ completes}]$ . An example of this in practice is found in Figure 8 and corresponding pseudo-code in Algorithm 1.

Computing the MST takes  $O(n \log n)$  time and cannot be computed in constant time for every CNOT gate, scaling with the size of the grid. We instead compute the MST of the grid every  $k$  cycles and use the latest computed MST. For example, if computing the MST takes  $\tau_{MST} = 50$  cycles and we set  $k = 25$  and the MST computation begins at  $t = 0$ , the MST would be computed only by time  $t = 50$ . Therefore, the ancilla activity information obtained from the MST would be *stale* by 50 cycles. In addition to this, two more MST computations would be running in parallel, one that started at  $t = 25$  and another

that begins at  $t = 50$ . Figure 9 gives an example execution of the MST computation process. However, we show in Section V-B3, this delay information has negligible effect on the performance of the dynamic compiler. We also provide a more detailed overhead analysis in Section V-D1.

## V. EVALUATION

### A. Benchmarks and Experimental Setup

Suite	Benchmarks	#Qubits	#Rz	#CNOT
large	ising	34	83	66
		42	103	82
		66	163	130
		98	243	194
		420	1048	838
	multiplier	45	2237	2286
		75	6384	6510
		29	708	680
	qft	63	1898	1836
		160	5293	5134
39		411	296	
qugan	71	763	552	
	111	1203	872	
medium	gcm	13	1528	762
	dnn	16	2432	384
	qft	18	323	306
	wstate	27	156	52
	HamiltonianSimulation	25	49	48
supermarq	HamiltonianSimulation	50	99	98
	QAOAFermionicSwap	75	149	148
	QAOAVanilla	15	120	315
	VQE	15	120	210
	VQE	13	78	12

TABLE III: List of the benchmarks for which we evaluate our dynamic compilation framework against the baseline implementations. The large and medium benchmark suites are from QASMBench [21]. We also evaluate on benchmarks from SupermarQ [33].

Table III lists the benchmarks (from QASMBench [21] and SupermarQ [33]) that we evaluate our compilation

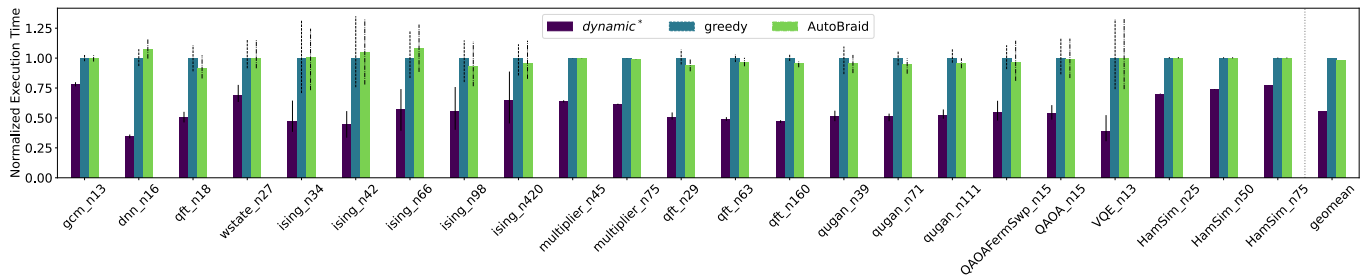


Fig. 10: Normalized average execution time for our compilation scheme versus the baseline schemes. The code distance was chosen to be 7 and the physical qubit error rate was chosen to be  $10^{-4}$ . We compute the execution time for  $k \in \{25, 50, 100, 200\}$  and report the best average execution time as *dynamic\**. The error bars between the minimum and maximum execution times are shown in black. We also report the geometric mean across all the benchmarks.

scheme on. These benchmarks were chosen as a representative set from QASMBench (*medium* and *large* suites) and Supermarq since these benchmarks span a large range of Rz gate to CNOT gate ratio ( $\approx 1 - 6.5$ ) and number of qubits (from 13 qubits to 420 qubits). In addition to this, these benchmarks also represent wide range of gate densities. For example, *wstate* and *qft* circuits are largely sequential while *ising* circuits are largely parallel. Most importantly, these benchmarks are chosen because they contain small angle rotations in the given representation. Other benchmarks which contain only deterministically prepared gates, e.g. Clifford’s only will behave identically in the static and dynamic cases.

1) *Sensitivity to the Code Distance*: We compile each benchmark into the basis gate set of  $Rz$ ,  $H$ ,  $X$  and CNOT using Qiskit [27] and report the total number of gates and the number of  $Rz$  and CNOT gates in the compiled version. We perform a one-to-one mapping of program qubits to logical qubits since gates in the benchmarks were between qubits of numerically close indices. We use the greedy path selection [18] and AutoBraid [16] as the baseline compilation schemes, and add edge-rotation gates if the chosen path requires an edge-rotation. We augment both schemes with the naive  $Rz$  gate preparation protocol; exactly one ancilla is reserved for preparing the  $|m_\theta\rangle$  state and early preparations are not done. We simulate each quantum program by choosing a random seed to model the preparation and injection probabilities and execution times as a function of the code distance and physical qubit error rate [1]. We then perform symbolic execution of the program to simulate the total execution time, accounting for delays due to non-deterministic failures, qubit stalls (both by ancilla and data qubits) and routing congestion. For each benchmark, we execute multiple times while varying the seed. For our dynamic protocol, we fix  $c$ , the number of cycles used to determine the ancilla activity to be 100 and evaluate the execution for the MST computation frequency,  $k \in \{25, 50, 100, 200\}$  cycles. Based on realistic grid sizes and estimates from MST computation time on modern CPUs, it takes about

$100\mu s$  (refer Section V-D1) to compute the MST. Since a lattice surgery cycle takes about  $1\mu s$  [23], the time taken to compute the MST is  $\tau_{MST} = 100$  lattice surgery cycles. We compare the performance of our dynamic compilation versus the baseline compilation schemes in Figure 10 and observe considerable performance improvements with a geomean of  $2\times$  speedup.

### B. Sensitivity Analysis

We evaluate our dynamic compilation framework against the baseline schemes for a large number of different code distances (Figure 11), physical qubit error rates (Figure 12) and also analyze how performance for our dynamic framework is affected with different  $k$  on changing  $p$  and  $d$  (Figure 13). We report the execution times and the fraction of time each data qubit remains idle for different benchmarks and the distribution across all benchmarks. Specifically, we report the performance on *dnn\_n16*, *gcm\_n13* and *qft\_n160* as representative benchmarks. These benchmarks were chosen based on the ratio of the  $Rz$  gates to the CNOT gates. *dnn\_n16* has a  $Rz$  to CNOT ratio of about 6:1, the largest among all benchmarks, *gcm\_n13* has a  $Rz$  to CNOT ratio of about 2:1 and *qft\_n160* has a  $Rz$  to CNOT ratio of 1:1. Finally, *qft\_n160* has 160 qubits, therefore, we also show how our compiler scales with more qubits. For both Figure 11 and Figure 12, we set  $k = 25$  for the dynamic compiler as indicated by *dynamic*<sub>25</sub>.

1) *Sensitivity to the Code Distance*: Figure 11 shows the performance of our compilation framework against the baselines as the code distance is changed. We fix  $p = 10^{-4}$ . The execution time improves as  $d$  is increased for all benchmarks and all compilers. We perform  $d$  rounds of syndrome measurements in every lattice surgery cycle and therefore the time taken for one measurement is  $1/d$ . The time taken for a single RUS attempt for preparation is a multiple of this fraction. With larger code distances, the number of RUS attempts for each lattice surgery cycle increase, improving the execution time. However, the execution time begins to saturate for  $d \geq 9$  and

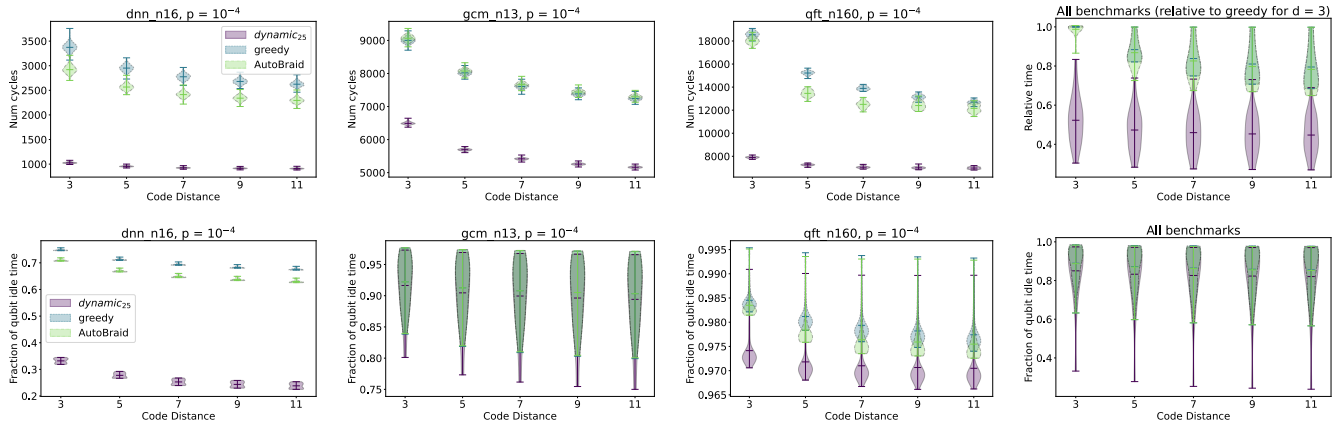


Fig. 11: Sensitivity of different compilation schemes to changing the code distance

is more or less the same for our dynamic compilation scheme irrespective of the code distance. This is because in the dynamic protocol, parallel preparation of the  $|m_\theta\rangle$  state almost guarantees that the RUS protocol succeeds within the first parallel attempt. Eager preparation of the correction state ensures we do not stall the data qubit in the case of injection failure, leading to our dynamic scheme being largely insensitive to the code distance. The same is also true for the fraction of time each data qubit spends idling.

2) *Sensitivity to the Physical Qubit Error Rate:* We plot the performance of the compilers relative to different physical qubit error rates in Figure 12. Similar to the sensitivity of the baselines to changing code distances, the baselines are highly sensitive to decreasing physical qubit error rates. Smaller  $p$  reduces the expected number of RUS attempts needed to successfully obtain the  $|m_\theta\rangle$  state. However, compared to the sensitivity of code distance, the sensitivity of both baselines and our dynamic compiler is lesser. This also holds true for the sensitivity of the idling time when changing  $p$  for the same reasons.

3) *Sensitivity to MST Computation Frequency:* Figure 13 shows the sensitivity of the dynamic compilation framework to the code distance and physical qubit error rate for  $k \in \{25, 50, 100, 200\}$ . For all the benchmarks, the sensitivity to both  $p$  and  $d$  is unaffected by  $k$  and the trend remains the same. Across different values of  $k$ , the performance is the best when  $k = 25$  and only slightly worsens as  $k$  is increased, however, the difference is negligible and the violin plots almost overlap for all  $k$ . Even though computing the MST less frequently will cause the same paths to be overused, this will not hinder the performance significantly since Algorithm 1 chooses between 16 (out of which 4 paths do not require any edge-rotation gates) possible different paths, distributing the load across different ancillas for CNOTs between the same pairs of qubits if ancillas become overused.

### C. Hardware-Software Co-Design

As discussed in Section II-B, the default STAR grid uses  $2 \times 2$  blocks for each data qubit, thus, there are 3 ancilla qubits for each data qubit. This overhead of ancilla resources is significant and we would want to reduce the number of ancilla qubits used by replacing some of the  $2 \times 2$  blocks with smaller blocks. We explore the trade-off for reducing the number of ancillas in the grid by incrementally *compressing* the grid by choosing a data qubit at random and modifying its patch from a  $2 \times 2$  to a  $2 \times 1$  patch until all data qubits have been *compressed*. We retain a column of ancillas at the extreme right of the grid to ensure that the entire grid still remains connected. We evaluate the compilation schemes for 0% ancilla reduction (3 ancilla per data), to 100% compression, where we have 1 ancilla per data, at increments of 25% compression. We report the results obtained in Figure 14. Similar to the plots discussed in Section V-B, we report the results on the three benchmarks and the relative execution time for both baselines and *dynamic*<sub>25</sub>.

The grid compression significantly affects the performance of the baseline schemes since both baseline protocols assume no congestion in the sub-grid that connects the control and target qubits for CNOT gate. In addition to this, the baseline schemes do not account for edge-rotation gates when choosing optimal paths. Thus, in benchmarks like gcm, when the grid is compressed, the probability of the baseline schemes to choose paths that do not require edge-rotation gates becomes more likely, leading to slightly reduced execution times. However, performance for our dynamic compilation scheme is not strongly affected by increased demand for the limited ancilla resources. In contrast, for qft and dnn, the increased stalls due to congestion dominate, which leads to increased execution times on grid compression. This congestion problem is less apparent for our dynamic compilation scheme due to the efficient schedules generated by using the queues. Our dynamic compilation scheme performs significantly better

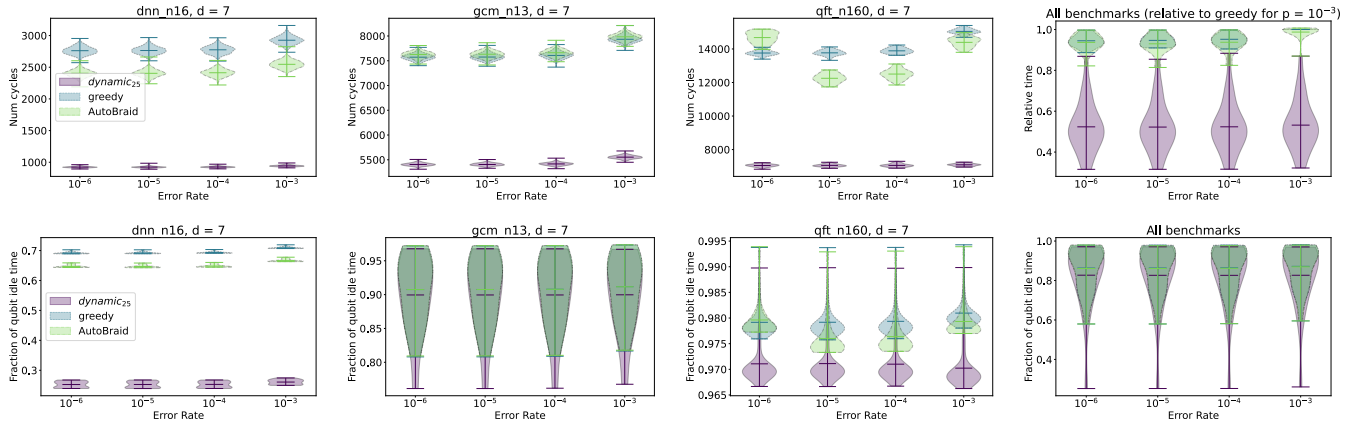


Fig. 12: Sensitivity of different compilation schemes to changing the physical qubit error rate

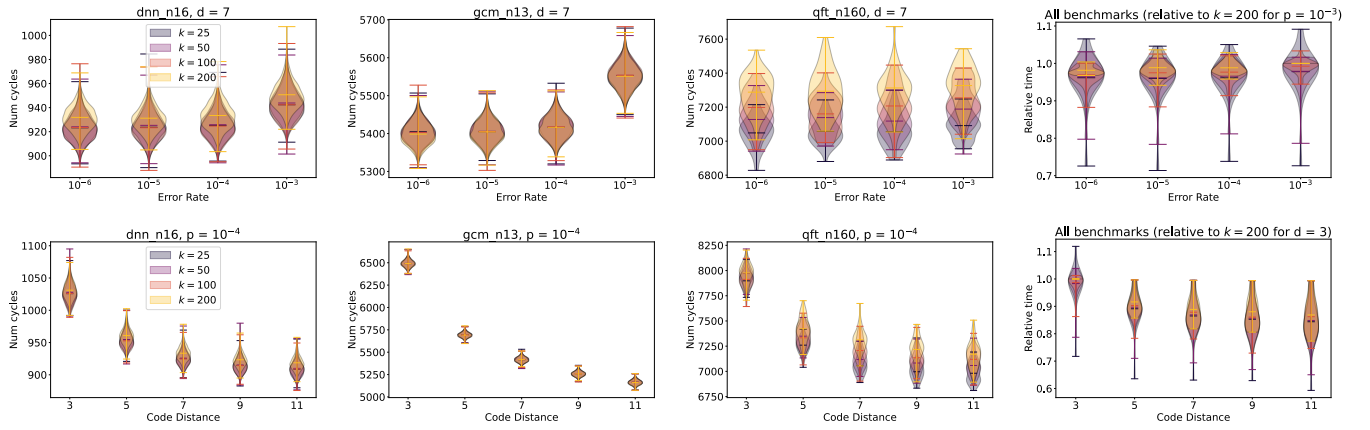


Fig. 13: Sensitivity of dynamic compilation scheme to changing  $d$  and  $p$  for different  $k$  (frequency of MST computation)

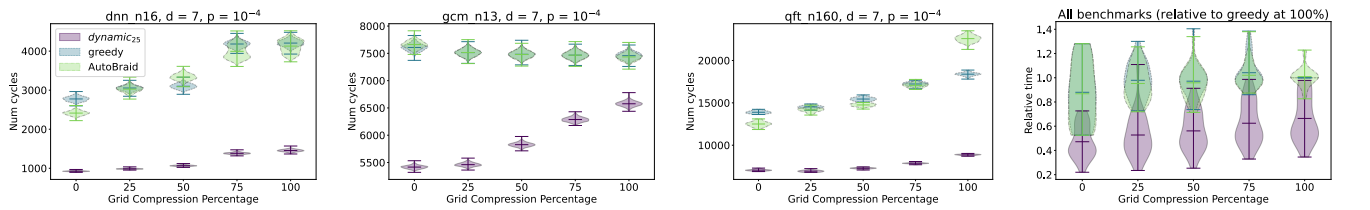


Fig. 14: Sensitivity of different compilation schemes to the ancilla availability

than the baseline schemes irrespective of the grid compression. The dynamic nature of our compiler is largely able to circumvent the stalls caused due to reduced ancilla resources, with only a small increase in relative execution times as the grid compresses.

#### D. Overheads of Classical Computation

We analyse and report the overhead of classical computation required for our compilation scheme. Note that the MST computation is performed asynchronously, i.e., the MST is computed independent of the quantum circuit execution.

1) *MST Computation Complexity*: Computing the MST on an arbitrary graph with  $n$  vertices takes  $O(n \log n)$  time [7]. We compute the MST over our proposed 2D grid architecture with some of the vertices absent (data qubits) since we only compute the MST on the ancilla qubits. This simplified graph makes it easier for us to instead perform updates on the MST rather than computing the entire MST from scratch. We have 4 cases for every edge  $a_{ij}$  out of which only two cases require MST updates:

- 1)  $a_{ij}$  is not on the MST and its activity decreases – we insert this edge to the MST and remove the largest

weight edge from the cycle formed. This will take  $O(1)$  time since all cycles are of  $O(1)$  size on a 2D grid.

- 2)  $a_{ij}$  is on the MST and its activity increases – we remove this edge from the MST and find the edge of least weight between the two forests. This step will take  $O(\max(\text{rows}, \text{columns}))$  since the edge removal will be along the horizontal or vertical direction.

Therefore, the time taken to update the MST will be of the  $O(\max(\text{rows}, \text{columns}))$  for each edge update. Since we have a square grid of  $n$  qubits and compute the MST every  $k$  cycles, there will only be  $O(k)$  edge updates and the overall time complexity simplifies to  $O(k\sqrt{n})$ . Based on our simulations and experiments on modern processors, it takes  $\approx 92\mu\text{s}$  for a  $100 \times 100$  grid and  $\approx 330\mu\text{s}$  for a  $1000 \times 1000$  grid when  $k = 200$ .

2) *Path-Finding Algorithm Complexity:* The path-finding algorithm uses the latest available MST and we always have at least one MST always available for the routing algorithm. All of the paths for the CNOT execution (line 16 of Algorithm 1) can also be computed on the MST and stored beforehand since they are independent of ancilla activity. Similarly, `startTime` can be updated whenever any ancilla on the path is used in some gate. This leads to only  $O(1)$  computation when the CNOT gate is being added to the queues: deciding the best path by comparing between `startTime` of the pre-computed paths.

## VI. CONCLUSION

Fault-tolerant quantum architectures are still far from being realized on physical systems. Various error correction techniques have been proposed, surface codes being one of them. The surface code architecture does not natively support non-Clifford gates and thus requires specialized support for such operations. Continuous rotation angle architectures have been proposed that allow for localized, low-latency ancilla preparation in the required states. However, this leads to the problem of supporting dynamic ancilla allocation to minimize runtime. Our work tackles this problem and we propose a dynamic compilation technique that utilizes the variable ancilla availability and activity to perform efficient allocation for different gate operations in parallel, thus minimizing the total program execution time. We improve significantly over the baseline proposals while simultaneously minimizing classical overhead for realtime recompilation.

## REFERENCES

- [1] Y. Akahoshi, K. Maruyama, H. Oshima, S. Sato, and K. Fujii, “Partially fault-tolerant quantum computing architecture with error-corrected clifford gates and space-time efficient analog rotations,” *arXiv preprint arXiv:2303.13181*, 2023.
- [2] J. T. Anderson, G. Duclos-Cianci, and D. Poulin, “Fault-tolerant conversion between the steane and reed-muller quantum codes,” *Physical review letters*, vol. 113, no. 8, p. 080501, 2014.
- [3] M. Beverland, V. Kliuchnikov, and E. Schoute, “Surface code compilation via edge-disjoint paths,” *PRX Quantum*, vol. 3, no. 2, p. 020342, 2022.
- [4] E. T. Campbell and M. Howard, “Unified framework for magic state distillation and multiqubit gate synthesis with reduced resource cost,” *Physical Review A*, vol. 95, no. 2, p. 022316, 2017.
- [5] E. T. Campbell and M. Howard, “Unifying gate synthesis and magic state distillation,” *Physical review letters*, vol. 118, no. 6, p. 060501, 2017.
- [6] H. Choi, F. T. Chong, D. Englund, and Y. Ding, “Fault tolerant non-clifford state preparation for arbitrary rotations,” *arXiv preprint arXiv:2303.17380*, 2023.
- [7] T. H. Cormen, C. E. Leiserson, R. L. Rivest, and C. Stein, *Introduction to Algorithms, Third Edition*, 3rd ed. The MIT Press, 2009.
- [8] Y. Ding, A. Holmes, A. Javadi-Abhari, D. Franklin, M. Martonosi, and F. Chong, “Magic-state functional units: Mapping and scheduling multi-level distillation circuits for fault-tolerant quantum architectures,” in *2018 51st Annual IEEE/ACM International Symposium on Microarchitecture (MICRO)*. IEEE, 2018, pp. 828–840.
- [9] Y. Ding, X.-C. Wu, A. Holmes, A. Wiseth, D. Franklin, M. Martonosi, and F. T. Chong, “Square: Strategic quantum ancilla reuse for modular quantum programs via cost-effective uncomputation,” in *2020 ACM/IEEE 47th Annual International Symposium on Computer Architecture (ISCA)*. IEEE, 2020, pp. 570–583.
- [10] B. Eastin and E. Knill, “Restrictions on transversal encoded quantum gate sets,” *Physical review letters*, vol. 102, no. 11, p. 110502, 2009.
- [11] A. G. Fowler, M. Mariantoni, J. M. Martinis, and A. N. Cleland, “Surface codes: Towards practical large-scale quantum computation,” *Physical Review A*, vol. 86, no. 3, sep 2012. [Online]. Available: <https://doi.org/10.1103/2Fphysreva.86.032324>
- [12] C. Gidney and M. Ekerå, “How to factor 2048 bit rsa integers in 8 hours using 20 million noisy qubits,” *Quantum*, vol. 5, p. 433, 2021.
- [13] O. Higgott, “Pymatching: A python package for decoding quantum codes with minimum-weight perfect matching,” *ACM Transactions on Quantum Computing*, vol. 3, no. 3, pp. 1–16, 2022.
- [14] A. Holmes, M. R. Jocar, G. Pasandi, Y. Ding, M. Pedram, and F. T. Chong, “Nisq+: Boosting quantum computing power by approximating quantum error correction,” *2020 ACM/IEEE 47th Annual International Symposium on Computer Architecture (ISCA)*, 2020. [Online]. Available: <https://par.nsf.gov/biblio/10211263>
- [15] D. Horsman, A. G. Fowler, S. Devitt, and R. Van Meter, “Surface code quantum computing by lattice surgery,” *New Journal of Physics*, vol. 14, no. 12, p. 123011, 2012.
- [16] F. Hua, Y. Chen, Y. Jin, C. Zhang, A. Hayes, Y. Zhang, and E. Z. Zhang, “Autobraid: A framework for enabling efficient surface code communication in quantum computing,” in *MICRO-54: 54th Annual IEEE/ACM International Symposium on Microarchitecture*, 2021, pp. 925–936.
- [17] S. Jandura and G. Pupillo, “Surface code stabilizer measurements for rydberg atoms,” *arXiv preprint arXiv:2405.16621*, 2024.
- [18] A. Javadi-Abhari, P. Gokhale, A. Holmes, D. Franklin, K. R. Brown, M. Martonosi, and F. T. Chong, “Optimized surface code communication in superconducting quantum computers,” in *Proceedings of the 50th Annual IEEE/ACM International Symposium on Microarchitecture*, ser. MICRO-50 ’17. New York, NY, USA: Association for Computing Machinery, 2017, p. 692–705. [Online]. Available: <https://doi.org/10.1145/3123939.3123949>
- [19] A. M. Kubica, “The abcs of the color code: A study of topological quantum codes as toy models for fault-tolerant quantum computation and quantum phases of matter,” Ph.D. dissertation, California Institute of Technology, 2018.
- [20] T. LeBlond, R. S. Bennink, J. G. Lietz, and C. M. Seck, “Tiscc: A surface code compiler and resource estimator for trapped-ion processors,” in *Proceedings of the SC’23 Workshops of The International Conference on High Performance Computing, Network, Storage, and Analysis*, 2023, pp. 1426–1435.
- [21] A. Li, S. Stein, S. Krishnamoorthy, and J. Ang, “Qasmbench:

- A low-level qasm benchmark suite for nisq evaluation and simulation,” 2022.
- [22] G. Li, Y. Ding, and Y. Xie, “Tackling the qubit mapping problem for nisq-era quantum devices,” in *Proceedings of the twenty-fourth international conference on architectural support for programming languages and operating systems*, 2019, pp. 1001–1014.
  - [23] D. Litinski, “A game of surface codes: Large-scale quantum computing with lattice surgery,” *Quantum*, vol. 3, p. 128, 2019.
  - [24] D. Litinski, “Magic state distillation: Not as costly as you think,” *Quantum*, vol. 3, p. 205, 2019.
  - [25] A. Molavi, A. Xu, S. Tannu, and A. Albarghouthi, “Compilation for surface code quantum computers,” *arXiv preprint arXiv:2311.18042*, 2023.
  - [26] P. Murali, J. M. Baker, A. Javadi-Abhari, F. T. Chong, and M. Martonosi, “Noise-adaptive compiler mappings for noisy intermediate-scale quantum computers,” in *Proceedings of the twenty-fourth international conference on architectural support for programming languages and operating systems*, 2019, pp. 1015–1029.
  - [27] Qiskit contributors, “Qiskit: An open-source framework for quantum computing,” 2023.
  - [28] G. S. Ravi, J. M. Baker, A. Fayyazi, S. F. Lin, A. Javadi-Abhari, M. Pedram, and F. T. Chong, “Better than worst-case decoding for quantum error correction,” in *Proceedings of the 28th ACM International Conference on Architectural Support for Programming Languages and Operating Systems, Volume 2*, 2023, pp. 88–102.
  - [29] N. J. Ross and P. Selinger, “Optimal ancilla-free clifford+ t approximation of z-rotations,” *arXiv preprint arXiv:1403.2975*, 2014.
  - [30] N. J. Ross and P. Selinger, “Optimal ancilla-free clifford+t approximation of z-rotations,” *Quantum Info. Comput.*, vol. 16, no. 11–12, p. 901–953, sep 2016.
  - [31] S. Sethi and J. Baker, <https://github.com/5ayam5/Realtime-Compilation-for-Continuous-Angle-QEC-Architectures>, 2024.
  - [32] S. S. Tannu and M. K. Qureshi, “Not all qubits are created equal: A case for variability-aware policies for nisq-era quantum computers,” in *Proceedings of the twenty-fourth international conference on architectural support for programming languages and operating systems*, 2019, pp. 987–999.
  - [33] T. Tomesh, P. Gokhale, V. Omole, G. Ravi, K. N. Smith, J. Vizslai, X. Wu, N. Hardavellas, M. R. Martonosi, and F. T. Chong, “Supermarq: A scalable quantum benchmark suite,” in *2022 IEEE International Symposium on High-Performance Computer Architecture (HPCA)*. Los Alamitos, CA, USA: IEEE Computer Society, apr 2022, pp. 587–603. [Online]. Available: <https://doi.ieeecomputersociety.org/10.1109/HPCA53966.2022.00050>
  - [34] J. Vizslai, S. F. Lin, S. Dangwal, J. M. Baker, and F. T. Chong, “An architecture for improved surface code connectivity in neutral atoms,” *arXiv preprint arXiv:2309.13507*, 2023.
  - [35] G. Watkins, H. M. Nguyen, K. Watkins, S. Pearce, H.-K. Lau, and A. Paler, “A high performance compiler for very large scale surface code computations,” *Quantum*, vol. 8, p. 1354, 2024.
  - [36] A. Wu, G. Li, H. Zhang, G. G. Guerreschi, Y. Ding, and Y. Xie, “A synthesis framework for stitching surface code with superconducting quantum devices,” in *Proceedings of the 49th Annual International Symposium on Computer Architecture*, 2022, pp. 337–350.